

2013

# Smaller, faster stomata: scaling of stomatal size, rate of response, and stomatal conductance

Paul Drake

Raymond H. Froend  
*Edith Cowan University*, [r.froend@ecu.edu.au](mailto:r.froend@ecu.edu.au)

Peter Franks

## **Smaller, faster stomata: Scaling of stomatal size, rate of response and stomatal conductance**

Paul L. Drake<sup>1</sup>, Ray H. Froend<sup>2</sup> and Peter J. Franks<sup>3</sup>

<sup>1</sup>Natural Resources Branch, Department of Environment and Conservation, Locked Bag 104, Bentley Delivery Centre, WA 6983, Australia

<sup>2</sup>School of Natural Sciences, Edith Cowan University, 270 Joondalup Drive, Joondalup, WA 6027, Australia 6027

<sup>3</sup>Faculty of Agriculture and Environment, University of Sydney, Sydney, NSW 2006

Author for correspondence: Peter Franks

Phone: +61 2 8627 1051

Fax: +61 2 8627 1099

Email: peter.franks@sydney.edu.au

Running title: Scaling of stomatal traits

Words: 3, 913 (body)

Tables: 2

Figures: 9

## ABSTRACT

Maximum and minimum stomatal conductance, as well as stomatal size and rate of response, are known to vary widely across plant species, but the functional relationship between these static and dynamic stomatal properties is unknown. Our objective was to test three hypotheses: (i) operating stomatal conductance under standard conditions ( $g_{op}$ ) correlates with minimum stomatal conductance prior to morning light, ( $g_{min(dawn)}$ ); (ii) stomatal size ( $S$ ) is negatively correlated with  $g_{op}$  and the maximum rate of stomatal opening in response to light,  $(dg/dt)_{max}$ ; (iii)  $g_{op}$  correlates negatively with instantaneous water-use efficiency (WUE) despite positive correlations with maximum rate of carboxylation ( $V_{cmax}$ ) and light-saturated rate of electron-transport ( $J_{max}$ ). Using five closely related species of the genus *Banksia*, we measured the above variables and found that all three hypotheses were supported by the results. Overall, this suggests that leaves built for higher rates of gas exchange have smaller stomata and faster dynamic characteristics. With the aid of a stomatal control model we demonstrate that higher  $g_{op}$  can potentially expose plants to larger tissue water potential gradients, and that faster stomatal response times can help offset this risk.

Key words: stomatal size, maximum stomatal conductance, night-time conductance, transpiration, stomatal control, water-use efficiency

26 INTRODUCTION

27

28 Plants regulate stomatal conductance to optimise carbon uptake with respect to water  
29 loss (Cowan, 1977; Farquhar *et al.*, 1980). An important limitation in this process is  
30 the rate at which stomata open in the light or close under darkness or water deficit  
31 (Cowan, 1977; Hetherington and Woodward 2003; Franks and Farquhar 2007;  
32 Brodribb *et al.*, 2009; Lawson *et al.*, 2011, Vico *et al.*, 2011). However, although  
33 stomatal response times are known to vary widely across species (Assmann and  
34 Grantz 1990; Franks and Farquhar 2007; Vico *et al.*, 2011), the biophysical factors  
35 governing the rate of response are not well understood.

36 Plant photosynthetic productivity and water-use efficiency also are linked to  
37 the dynamic range of stomatal conductance. Under favourable conditions of low  
38 evaporative demand and high light, productivity is constrained by the maximum  
39 operating stomatal conductance,  $g_{op}$ , and under severe water deficits resulting from  
40 high evaporative demand and/or dry soil, plants rely upon full stomatal closure and a  
41 highly water-impermeable leaf cuticle to minimise water loss (Hinckley *et al.*, 1980;  
42 McDowell *et al.*, 2008). Across plant taxa there is a wide range of operating and  
43 minimum stomatal conductances (Jones, 1992; Schulze *et al.*, 1994; Körner, 1995).  
44 However, it is not known if maximum and minimum stomatal conductance typically  
45 scale with one another.

46 Commonly defined as the minimum stomatal conductance in darkness,  $g_{min}$  for  
47 a given leaf may differ on account of the time of day or other physiological  
48 circumstances. For example, stomata typically close in response to darkness and  
49 remain so for much of the night, but often the closure is not complete. In fact the  
50 night-time or 'nocturnal' conductance can be sufficient to allow significant  
51 transpiration (Ehrler, 1971; Benyon, 1999; Snyder, *et al.*, 2003; Barbour *et al.*, 2005;  
52 Bucci *et al.*, 2005; Daley and Phillips, 2006; Dawson *et al.*, 2007), and growth  
53 conditions may produce stomata that cannot close completely even when fully  
54 deflated at zero turgor (Franks and Farquhar, 2007). Night-time transpiration rates  
55 are typically between 5% to 15% of daytime transpiration, but in rare cases can be  
56 more than 30% (Caird *et al.*, 2007; Novick *et al.*, 2009). Such high rates of water loss  
57 at times of little or no carbon gain are inconsistent with the general role of stomata as  
58 a water conserving apparatus, but little is known about the mechanism of nocturnally  
59 elevated stomatal conductance or its relationship to the minimum conductance in

60 darkness at other times of the day and under desiccation. Here we distinguish  
61 between three different conductance minima according to the circumstances in which  
62 they are promoted: (i)  $g_{\min(\text{dawn})}$ , referring to the minimum stomatal conductance to  
63 water vapour at the end of the nocturnal dark phase; (ii)  $g_{\min(\text{day})}$ , referring to the  
64 minimum stomatal conductance to water vapour attained when the leaf is exposed to a  
65 period of darkness during to normal daylight hours; (iii) the absolute minimum  
66 conductance to water vapour,  $g_{\min(\text{abs})}$ , occurring when the guard cells are fully  
67 deflated as a result of complete turgor loss (Fig. 1). The quantities  $g_{\text{op}}$ ,  $g_{\min(\text{dawn})}$ ,  
68  $g_{\min(\text{day})}$ , and  $g_{\min(\text{abs})}$  all comprise a stomatal component in parallel with a cuticular  
69 component, although  $g_{\min(\text{abs})}$  may closely approximate cuticular conductance.  
70 Common empirical stomatal models do not adequately account for elevated minimum  
71 conductance at night or its environmental sensitivities (Barbour and Buckley, 2007)  
72 but few studies have measured all of these conductances together so the relationship  
73 between them is obscure.

74         The operating stomatal conductance,  $g_{\text{op}}$ , is also known to scale with other leaf  
75 gas exchange and water transport attributes, such as  $\text{CO}_2$  assimilation rate and leaf  
76 hydraulic conductance (Meinzer, 2003; Brodribb *et al.*, 2007). However,  
77 nonlinearities in some of these relationships result in trade-offs. For example,  
78 increased  $\text{CO}_2$  assimilation rate accompanying higher  $g_{\text{op}}$  may be associated with  
79 lower water-use efficiency (Franks and Farquhar, 1999) and higher leaf water  
80 potential gradients (Franks, 2006). Improved stomatal dynamic properties with  
81 increased  $g_{\text{op}}$  could potentially help to offset these counterproductive properties.

82         The operating conductance  $g_{\text{op}}$  is constrained by the maximum stomatal  
83 conductance,  $g_{\text{max}}$ , which in turn is determined by two physical attributes of stomata,  
84 (i) their size ( $S$ ) and (ii) their density ( $D$ ), or number per unit area. We distinguish  
85 between  $g_{\text{max}}$  and  $g_{\text{op}}$  because  $g_{\text{max}}$  relates to stomata opened to their widest possible  
86 apertures (e.g. under 100% relative humidity and low ambient  $\text{CO}_2$  concentration),  
87 whereas under typical operating conditions (less than 100% relative humidity and  
88 normal ambient  $\text{CO}_2$  concentration) stomatal apertures will be less than fully open. It  
89 has been shown that across broad geological timescales and evolutionary lineages  
90 higher  $g_{\text{max}}$  and  $g_{\text{op}}$  are associated with smaller stomatal size and higher density, and  
91 that  $S$  is negatively correlated with  $D$  (Hetherington and Woodward, 2003; Franks and  
92 Beerling, 2009). This relationship has also been found to apply within a single  
93 species across environmental gradients (Franks *et al.*, 2009), and also across a group

94 of six tree species of different genus (Aasama *et al.*, 2001). Smaller stomata, due to  
95 their greater membrane surface area to volume ratio, may have faster response times  
96 compared to larger stomata, and this in combination with high stomatal density may  
97 allow the leaf to attain high  $g_{op}$  rapidly under favorable conditions, and to rapidly  
98 reduce conductance when conditions are unfavorable. In such a system, the rate of  
99 stomatal response would be positively correlated with  $g_{op}$  and negatively correlated  
100 with stomatal size. However, to date, these functional relationships have not been  
101 confirmed.

102 Our objective was to test three hypotheses: (i) operating stomatal conductance  
103 under standard conditions ( $g_{op}$ ) correlates with minimum stomatal conductance prior  
104 to morning light, ( $g_{min(dawn)}$ ); (ii) stomatal size ( $S$ ) is negatively correlated with  $g_{op}$   
105 and the maximum rate of stomatal opening in response to light,  $(dg/dt)_{max}$ ; (iii)  $g_{op}$   
106 correlates negatively with instantaneous water-use efficiency (WUE) despite positive  
107 correlations with maximum rate of carboxylation ( $V_{cmax}$ ) and light-saturated rate of  
108 electron-transport ( $J_{max}$ ). To test our hypotheses we measured the above traits in a  
109 closely related group of *Banksia* species that are distributed across a broad  
110 hydrological environment from wetlands to dune crests (Fig. 2) (Groom, 2002;  
111 Groom, 2004). Restricting the study to a single genus ensured minimal genetic  
112 variability while offering a broad range of  $g_{op}$ , stomatal size and stomatal density  
113 traits for analysis. The results are assessed in terms of their implications for plant  
114 water balance and fitness under the differing hydrological habitats of the study  
115 species.

116

## 117 MATERIALS AND METHODS

118

### 119 *Plant material*

120

121 Five *Banksia* species, endemic to the *Banksia* woodland of south-western Australia  
122 (31°45' S, 115°57' E), were selected for study. The species were as follows: *Banksia*  
123 *attenuata* R.Br., *Banksia menziesii* R.Br., *Banksia ilicifolia* R.Br., *Banksia prionotes*  
124 Lindl. and *Banksia littoralis* R.Br. Figure 2, based on the natural geographical range  
125 of south-west Australian banksias, is an idealised representation of the distribution of  
126 the species across five distinct habitats as defined by the depth of groundwater from  
127 the natural surface (Table 1).

128 Four plants from each species were grown from seed in a glasshouse in 10 L  
129 pots. Plants were allowed to develop in 70:30 coarse sand:humus and fertilized with  
130  $33.38 \pm 0.24$  grams (mean  $\pm$  SE) of slow release fertilizer (Osmocote™). All plants  
131 were well watered throughout development and maintained under a day/night  
132 temperature regime of 24/15°C. When leaves had fully matured under these  
133 conditions, each plant was periodically transferred to a laboratory (air temperature  
134 range =  $23 \pm 3^\circ\text{C}$ ), rewatered and allowed to equilibrate overnight in preparation for  
135 the following day's gas exchange measurements.

136

### 137 *Gas exchange*

138

139 Leaf gas exchange properties were measured in the laboratory with an open-flow  
140 portable photosynthesis system (Model Li 6400, Li-cor Inc, Lincoln, Nebraska) on  
141 one leaf per plant ( $n = 4$  plants per species). All experiments were initiated early in  
142 the morning (07:30 – 08:30 local standard time) and were concluded within the  
143 natural daylight photoperiod. Plants were kept well watered throughout  
144 measurements. Measurements were made on fully expanded leaves (three or four  
145 leaves back from a branch apex). Throughout experiments the ambient mole fraction  
146 of  $\text{CO}_2$  ( $c_a$ ) was maintained at  $350 \mu\text{mol CO}_2 \text{ mol}^{-1}$  air (except for relationships  
147 between assimilation rate ( $A$ ) and intercellular mole fraction of  $\text{CO}_2$  ( $c_i$ )), leaf  
148 temperature was set at  $20^\circ\text{C}$  and leaf-to-air vapour pressure difference regulated to 1  
149 kPa.

150 In the morning, minimum steady-state stomatal conductance to water vapour  
151 prior to light exposure ( $g_{\min(\text{dawn})}$ ,  $\text{mol H}_2\text{O m}^{-2} \text{ leaf s}^{-1}$ ) was determined with the leaf  
152 in darkness. A stomatal opening phase, comprising the transition from  $g_{\min(\text{dawn})}$  to a  
153 maximum steady-state or operating stomatal conductance to water vapour ( $g_{\text{op}}$ ,  $\text{mol}$   
154  $\text{H}_2\text{O m}^{-2} \text{ leaf s}^{-1}$ ), was then recorded by exposing leaves to a photosynthetically active  
155 radiation (PAR) of  $1500 \mu\text{mol m}^{-2} \text{ s}^{-1}$  (while keeping the other chamber conditions  
156 constant) and logging instantaneous stomatal conductance ( $g$ ) at 60 second intervals.  
157 This opening phase took approximately 120 minutes to reach a steady-state  $g_{\text{op}}$  for  
158 each species. After ensuring that all transient stomatal opening had ceased, the  
159 maximum steady-state  $\text{CO}_2$  assimilation rate ( $A_{\text{op}}$ ,  $\mu\text{mol m}^{-2} \text{ leaf s}^{-1}$ ) and  
160 corresponding intercellular  $\text{CO}_2$  mole fraction ( $c_{i(\text{op})}$ ,  $\mu\text{mol CO}_2 \text{ mol}^{-1}$  air) and steady-

161 state transpiration rate ( $E_{op}$ , mmol H<sub>2</sub>O m<sup>-2</sup> leaf s<sup>-1</sup>) were also recorded. Also at this  
 162 point, the relationship between instantaneous CO<sub>2</sub> assimilation rate  $A$  and leaf  
 163 intercellular CO<sub>2</sub> concentration  $c_i$  was obtained (see below). Photosynthetically  
 164 active radiation was then returned to zero and the subsequent stomatal closing phase,  
 165 to a minimum steady-state value,  $g_{\min(\text{day})}$ , was recorded by logging stomatal  
 166 conductance at 60 second intervals. The timeframe for stomatal closure varied across  
 167 species, ranging from approximately 100 to 250 minutes. The leaf was then excised  
 168 from the plant and any further decline in stomatal conductance recorded, with the  
 169 final minimum conductance for excised leaves measured as the absolute minimum,  
 170  $g_{\min(\text{abs})}$ .

171 The relationship between  $A$  and  $c_i$  was obtained for each plant by manipulating  
 172  $c_a$  over the range 50 μmol CO<sub>2</sub> mol<sup>-1</sup> air to 2000 μmol CO<sub>2</sub> mol<sup>-1</sup> air, beginning with  
 173 the steady state conditions at 350 μmol CO<sub>2</sub> mol<sup>-1</sup> air, then stepping  $c_a$  down to 300,  
 174 200, 100, 50 and then up to 400, 600, 800, 1000, 1400, 1800 and 2000 μmol CO<sub>2</sub> mol<sup>-1</sup>  
 175 air. We characterised the relationship according to the model proposed by Farquhar  
 176 *et al.* (1980) and subsequently modified by von Caemmerer and Farquhar (1981),  
 177 Sharkey (1985) and Harley *et al.* (1992). Undertaking this mechanistic analysis of the  
 178 relationship between  $A$  and  $c_i$  yielded estimates for the maximum rate of  
 179 carboxylation ( $V_{c_{\max}}$ , μmol CO<sub>2</sub> m<sup>-2</sup> leaf s<sup>-1</sup>) and the light saturated rate of electron  
 180 transport ( $J_{\max}$ , μmol CO<sub>2</sub> m<sup>-2</sup> leaf s<sup>-1</sup>).

181

182 *Deriving the maximum rate of stomatal opening*

183

184 Plots of instantaneous stomatal conductance ( $g$ ) versus time elapsed since the start of  
 185 measurements ( $t$ , seconds) obtained during the stomatal opening phase were described  
 186 by Boltzmann sigmoidal models:

187

$$188 \quad g = \frac{a_1 - a_2}{1 + e^{-t-t_0/dt'}} + a_2 \quad (1)$$

189

190 where  $a_1$  (mol m<sup>-2</sup> s<sup>-1</sup>) is the left horizontal asymptote,  $a_2$  (mol m<sup>-2</sup> s<sup>-1</sup>) is the right  
 191 horizontal asymptote,  $t_0$  (seconds) is the point of inflection and  $dt'$  (seconds) is the  
 192 change in time that corresponds to the greatest change in  $g$ . Using an iterative least



193 squares fit approach, values for  $a_1$ ,  $a_2$ ,  $t_0$  and  $dt'$  were determined for each plant. The  
194 instantaneous rates of stomatal opening ( $dg/dt$ , mol m<sup>-2</sup> s<sup>-2</sup>) across the entire range of  $t$   
195 were then calculated by taking the derivative of Equation 1:

$$\frac{dg}{dt} = \frac{e^{(t_0+t)/dt'} (a_2 - a_1)}{(e^{t_0/dt'} + e^{t/dt'})^2 dt'}$$

197 (2)

198  
199 and the maximum rate of stomatal opening ( $dg/dt_{\max}$ , mol m<sup>-2</sup> s<sup>-2</sup>) determined for each  
200 plant as  $dg/dt$  when  $t = t_0$ .

201  
202 This procedure was repeated after converting  $g$  to a relative value,  $g_{\text{relative}}$ :

$$g_{\text{relative}} = \frac{g - g_{\min(\text{dawn})}}{g_{\text{op}} - g_{\min(\text{dawn})}}$$

203 (3)

204 and the time taken to reach 50% of  $g_{\text{relative}}$  ( $t_{50}$ , minutes) determined.

205

### 206 *Stomatal morphology*

207

208 A tissue sample was obtained halfway from the leaf tip to the base from each leaf that  
209 was analysed for gas exchange properties and stored in 70% ethanol. For all species  
210 except *B. littoralis*, stomata were concentrated within crypts on the abaxial surface.  
211 Stomata of *B. littoralis* also only occurred on the abaxial surface but no crypts were  
212 observed. The leaf epidermal surface of each species was also comprised of thickly  
213 intertwined trichomes. To obtain a clear view of stomata amidst these surface  
214 features, each sample was first rehydrated by rinsing under tap water then embedded  
215 in paraffin wax. Planar (through the epidermis) and transverse sections were then cut  
216 to 10 µm thickness with a rotary microtome (Leica model RM 2125, Leica  
217 Microsystems, Wetzlar, Germany). The sections were then positioned on slides that  
218 were dipped in 2% gelatin immediately prior to mounting. Slides were then placed in  
219 a coplin jar with filter paper soaked in formaldehyde to allow vapour fixation (of  
220 section to gelatin). The coplin jar was covered with a lid and the sections allowed to  
221 dry at room temperature for 12 hours. Sections were then stained in 0.1% aqueous

222 toluidine blue, examined under a compound light microscope and images captured  
223 with a digital camera.

224 Stomatal morphological parameters (guard cell length  $L$  ( $\mu\text{m}$ ) and guard cell  
225 pair width  $W$  ( $\mu\text{m}$ )) were measured from images obtained from planar sections as the  
226 mean of 20 stomatal complexes (guard cell pairs) for each species. We report stomatal  
227 size ( $S$ ) as the product of  $L$  and  $W$  ( $\mu\text{m}^2$ ).

228 For each species stomatal density, i.e. number of stomata per unit epidermal  
229 area ( $D$ ,  $\text{mm}^{-2}$ ) was calculated from transverse sections. For each section, the number  
230 of stomata ( $n_s$ ) intercepted by the microtome during cutting was counted along a  
231 known length of epidermis ( $l$ ,  $\mu\text{m}$ ,  $n = 12$  lengths per species). The length of  
232 epidermis ranged from approximately 450  $\mu\text{m}$  to 4400  $\mu\text{m}$ . Assuming each transect  
233 captured an area of epidermis of width ( $w_e$ ) approximately equal to the average of the  
234 length and width of a stoma, the stomatal density was calculated as  $D = n_s/(l \times w_e)$ .

235

## 236 RESULTS

237

238 The operating stomatal conductance  $g_{op}$  was positively correlated with  $g_{\min(\text{dawn})}$  ( $y =$   
239  $0.844 - 0.562e^{-(x - 0.004)/0.024}$ ,  $r^2 = 0.70$ , Fig. 3A) and with  $(dg/dt)_{\max}$  (Fig. 3B,  $y = -0.09$   
240  $+ 3.40x$ ,  $r^2 = 0.71$ ,  $P < 0.001$ ). Across species there was a three-fold variation in  
241  $(dg/dt)_{\max}$ , ranging from 0.07  $\text{mmol m}^{-2} \text{s}^{-2}$  to 0.25  $\text{mmol m}^{-2} \text{s}^{-2}$ .  $g_{\min(\text{dawn})}$  was also  
242 positively correlated with  $(dg/dt)_{\max}$  (Fig 3C,  $y = 5.08 \times 10^{-6}e^{(x/0.03)} + 0.01$ ,  $r^2 = 0.78$ ).  
243 These results indicate that higher maximum and minimum stomatal conductance is  
244 linked to faster absolute rates of response of stomatal stomatal conductance to leaf  
245 irradiance.

246 Stomatal size ( $S$ ) was negatively correlated with  $(dg/dt)_{\max}$  across species (Fig.  
247 4A,  $y = 15877.84 \times e^{(-x/0.03)} + 340.52$ ,  $r^2 = 0.88$ ,  $P < 0.01$ ) and stomatal density  $D$  was  
248 positively correlated with  $(dg/dt)_{\max}$  (Fig. 4B,  $y = 77.43 + 1643.06x$ ,  $r^2 = 0.71$ ,  $P <$   
249  $0.05$ ), indicating that leaves with smaller and more numerous stomata exhibit faster  
250 absolute rates of response of stomatal conductance to water vapour. The positive  
251 relationship between  $t_{50}$  and  $S$  (Fig. 4C,  $y = 16.63 + 0.05x$ ,  $r^2 = 0.34$ ,  $P < 0.05$ ) further  
252 indicates that smaller stomata exhibited a faster response in relative terms.

253 Stomatal opening in response to a step increase in light followed a similar  
254 pattern in all species, resembling the typical dynamic response of a second order

255 dynamic system with near-critical damping (Fig 5A-E). For each species the stomatal  
256 opening phase was accompanied by an increase in CO<sub>2</sub> assimilation rate (*A*) to a  
257 maximum steady-state value (*A*<sub>op</sub>), although *A*<sub>op</sub> was established prior to *g*<sub>op</sub> (Fig 5F-  
258 J).

259 Although *g*<sub>op</sub> varied by about five fold across species, *g*<sub>min(dawn)</sub> varied by 15  
260 fold (Table 2.). Across the five species, there was well over a two-fold range between  
261 highest and lowest mean species *g*<sub>op</sub> measured under controlled laboratory conditions.  
262 The mean absolute minimum stomatal conductance *g*<sub>min(abs)</sub> ranged from 6.0 to 20  
263 mmol m<sup>-2</sup> s<sup>-1</sup>, which compares favourably to the range of minimum stomatal  
264 conductance reported for deciduous and evergreen plants using leaf drying curves (1.0  
265 to 20 mmol m<sup>-2</sup> s<sup>-1</sup>) (Burghardt and Riederer, 2003).

266 Over the dynamic range of stomatal opening, CO<sub>2</sub> assimilation rate increased  
267 with stomatal conductance in the usual saturating fashion (Fig. 6A). Steady-state  
268 instantaneous water use-efficiency (WUE<sub>i</sub>), defined as *A*<sub>op</sub>/*E*<sub>op</sub> at 1 kPa VPD (see the  
269 controlled, standardised environmental conditions in Methods) ranged from 2.5 to 6.5  
270 mmol mol<sup>-1</sup> and all of the species reached a peak in WUE<sub>i</sub> when *A* was about 5 μmol  
271 m<sup>-2</sup> s<sup>-1</sup> (Fig. 6B). *B. attenuata* and *B. menzeisii* had the highest WUE<sub>i</sub> and *B. littoralis*  
272 had the lowest WUE<sub>i</sub> (Fig. 6B). Also, WUE<sub>i</sub> was negatively correlated with *g*<sub>op</sub> (Fig.  
273 6C;  $y = 6.49 - 4.51x$ ;  $r^2 = 0.52$ ,  $P < 0.001$ ).

274 The maximum rate of carboxylation (*V*<sub>C<sub>max</sub></sub>) ranged from 23.90 μmol m<sup>-2</sup> s<sup>-1</sup> to  
275 47.11 μmol m<sup>-2</sup> s<sup>-1</sup> and the light saturated rate of electron transport (*J*<sub>max</sub>) ranged from  
276 64.2 μmol m<sup>-2</sup> s<sup>-1</sup> to 131 μmol m<sup>-2</sup> s<sup>-1</sup>. The average value of *V*<sub>C<sub>max</sub></sub> and *J*<sub>max</sub> was 37.22  
277 ± 1.47 μmol m<sup>-2</sup> s<sup>-1</sup> and 103.74 ± 4.24 μmol m<sup>-2</sup> s<sup>-1</sup> respectively. This is lower than  
278 the average values reported by (Wullschleger SD, 1993) for sclerophyllous shrubs (53  
279 ± 15 μmol m<sup>-2</sup> s<sup>-1</sup> and 122 ± 31 μmol m<sup>-2</sup> s<sup>-1</sup> for *V*<sub>C<sub>max</sub></sub> and *J*<sub>max</sub> respectively), but is  
280 similar to the values for temperate forest hardwoods (47 ± 33 μmol m<sup>-2</sup> s<sup>-1</sup> and 104 ±  
281 67 μmol m<sup>-2</sup> s<sup>-1</sup> for *V*<sub>C<sub>max</sub></sub> and *J*<sub>max</sub> respectively). Across individual plants *A*<sub>(op)</sub>  
282 (defined here as the maximum operating CO<sub>2</sub> assimilation rate under standard  
283 conditions, as distinct from the maximum ribulose biphosphate regeneration limited  
284 rate induced under elevated CO<sub>2</sub> concentration) was positively correlated with *V*<sub>C<sub>max</sub></sub>  
285 (Fig. 7A) and *J*<sub>max</sub> (Fig. 7B) ( $y = 0.47x - 1.39$ ,  $r^2 = 0.81$ ,  $P < 0.001$  for *A*<sub>(op)(max)</sub> versus  
286 *V*<sub>C<sub>max</sub></sub> and  $y = 0.14x + 1.14$ ,  $r^2 = 0.64$   $P < 0.001$  for *A*<sub>(op)(max)</sub> versus *J*<sub>max</sub>). There was no  
287 apparent species grouping within either correlation.

288 Stomatal closure in response to darkening of leaves followed a similar pattern  
289 across species, but the minimum steady conductance during this midday darkening of  
290 leaves,  $g_{\min(\text{day})}$ , was considerably higher than  $g_{\min(\text{dawn})}$  (Fig. 8). The average  
291 percentage decline in  $g$  after midday darkening, with respect to the illuminated  
292 steady-state conductance ( $g_{\text{op}}$ ), was 59.23, 61.80, 64.36, 65.57 and 86.08 for *B.*  
293 *menziesii*, *B. prionotes*, *B. ilicifolia*, *B. attenuata*, and *B. littoralis* respectively. After  
294 excising leaves, a further decline in  $g$  was noted. The average percentage decline in  $g$   
295 with leaf excision, relative to  $g_{\min(\text{day})}$ , was 95.00, 93.28, 95.20, 94.87 and 79.93 for *B.*  
296 *attenuata*, *B. menziesii*, *B. ilicifolia*, *B. prionotes* and *B. littoralis* respectively. On  
297 this occasion *B. littoralis*, the species restricted to sites with high soil moisture,  
298 showed the least relative decline in  $g$ .

299

## 300 DISCUSSION

301

302 In support of hypotheses (i) and (ii),  $g_{\text{op}}$  correlated with  $g_{\min(\text{dawn})}$  and with the  
303 maximum rate of stomatal response to light,  $(dg/dt)_{\text{max}}$  (Fig. 3A, 3B). The results  
304 suggest that the day and night-time stomatal conductances are positively correlated  
305 across these *Banksia* species and that a functional connection exists between these  
306 traits and the dynamic behaviour of stomata. Enhanced dynamic response with  
307 higher operational stomatal conductance has implications for improved long-term  
308 water-use efficiency and lower risk of disruption of the leaf hydraulic system.

309 The positive correlation between  $g_{\text{op}}$  and  $g_{\min(\text{dawn})}$  (Fig. 3A) suggests that there  
310 is a trade-off in which leaves built for higher rates of leaf gas exchange maintain  
311 higher stomatal conductance at night. The positive correlation also between  $g_{\text{op}}$  and  
312  $(dg/dt)_{\text{max}}$  (Fig. 3B) suggests that the water losses due to the accompanying elevated  
313 night-time stomatal conductance and, consequently, the elevated night-time  
314 transpiration rates are offset by better dynamic control of stomata during the day.  
315 The role of night-time stomatal conductance remains elusive and the mechanism of its  
316 control is poorly understood (Barbour and Buckley, 2007). However, the scaling  
317 relationships identified in our study provide important mechanistic foundations for  
318 predicting the dynamic range of stomatal control and for improved modelling of  
319 stomatal control through day-night cycles.

320 Higher  $g_{\text{op}}$ , faster  $(dg/dt)_{\text{max}}$  and shorter  $t_{50}$  were associated with smaller and  
321 more numerous stomata (Fig. 4A-C). Investment in stomatal infrastructure to

322 facilitate high gas exchange capacity is constrained by the availability of space on the  
323 leaf surface and the total metabolic energy required to actively regulate stomatal pore  
324 size in a given number of stomata (Franks and Farquhar, 2007; Franks *et al.*, 2009).  
325 Our study suggests that the inherently faster stomatal response of leaves with high  $g_{op}$   
326 and smaller stomata could provide enhanced water balance in dynamic light  
327 environments in addition to the higher assimilation rates accompanying high  $g_{op}$ .  
328 However, the interaction between the dynamic response of stomata and the frequency  
329 of light fluctuations is complex, with frequency dramatically influencing the average  
330 stomatal response (Cardon *et al.*, 1994).

331         Despite the advantages of faster stomatal response (i.e. compared to leaves  
332 with the same  $g_{op}$  but slower stomatal response), greater overall water-use efficiency  
333 may still be more strongly associated with lower  $g_{op}$ , as suggested by the negative  
334 correlation between  $WUE_i$  and  $g_{op}$  across species (Fig 6C). However, the faster  
335 response times associated with higher  $g_{op}$  (Fig 3B, Fig 4C) help to compensate for  
336 this.  $WUE_i$  trended towards higher values in species that occur naturally in areas with  
337 a large depth to groundwater (Table 1) and therefore higher probability of water  
338 deficit. Assuming these qualities are genetically conserved and the observed  
339 differences translate qualitatively to these species in their natural environment, the  
340 results help to explain why the species with higher photosynthetic capacity prefer  
341 damp habitats while those with lower capacity occupy seasonally dry habitats (Fig. 2).  
342 Similarly, Anderson *et al.* (1996) showed that the water-use efficiency of commonly  
343 grown *Eucalyptus* species correlated negatively with the rainfall of their respective  
344 native habitat, suggesting genetic conservation of gas exchange traits that have been  
345 optimised to local conditions. Faster stomatal response improves water-use efficiency  
346 in environments with fluctuating light and evaporative demand, so higher  $(dg/dt)_{max}$   
347 associated with higher  $g_{op}$  will help to counteract reduced  $WUE_i$  in leaves with high  
348  $g_{op}$ .

349         The correlation between  $g_{op}$  and  $(dg/dt)_{max}$  is consistent with selection for a  
350 stomatal control mechanism that minimizes exposure to excessive water potential  
351 gradients. With increasing  $g_{op}$  the plant is more exposed to potentially damaging  
352 water potential gradients arising from sudden changes in evaporation potential. Faster  
353 stomatal closure in response to these changes will reduce the risks associated with  
354 such exposure, including formation of air embolisms in the xylem. Stomatal response  
355 to light and VPD (or transpiration rate) have similar kinetics (Grantz and Zeiger,

356 1986), so it may be useful to compare species on the basis of them having generally  
357 'faster' or 'slower' stomatal mechanisms. In Fig. 9 we illustrate the value of faster  
358 response times for plants with higher  $g_{op}$ . The simulations use the data and model in  
359 Franks (2006) for plants with different gas exchange and hydraulic capacities. It is  
360 shown that, for a step increase in VPD from 1 to 1.5 kPa, plants operating with higher  
361  $g_{op}$  at 1 kPa VPD are exposed to higher leaf water potential gradients ( $\Delta\Psi_{leaf}$ )  
362 immediately after the change, and may therefore benefit from a faster rate of  
363 reduction of stomatal conductance to the new steady rate at 1.5 kPa VPD.

364

### 365 *Conclusions*

366 Although several studies have demonstrated scaling of stomatal conductance with  
367 static indicators of plant gas exchange capacity (Wong et al.1979; Field and Mooney,  
368 1986; Meinzer, 2003), our results show scaling with a dynamic performance  
369 characteristic,  $(dg/dt)_{max}$ , and this dynamic attribute also scaled with stomatal size and  
370 stomatal density. Maximum daytime operating stomatal conductance,  $g_{op}$ , and pre-  
371 dawn minimum stomatal conductance,  $g_{min(dawn)}$ , were positively correlated with the  
372 rate of stomatal response to light. Leaves with higher  $g_{op}$  have lower instantaneous  
373 water-use efficiency and are exposed to larger transient water potential gradients.  
374 Faster stomatal response times in such leaves may improve long-term water-use  
375 efficiency and reduce exposure to transient water potential gradients. Smaller stomata  
376 with faster dynamic characteristics may therefore be integral to selection for high  
377 stomatal conductances accompanying higher photosynthetic capacity. This principle  
378 may also be applied in the selection for plants with improved agricultural qualities.

379

### 380 ACKNOWLEDGMENTS

381

382 We thank Robyn Loomes and Muriel Davies for maintaining the glasshouse and  
383 Gordon Thomson for assistance with histology. We are also grateful for helpful  
384 comments from Daniel Mendham. This project was supported by the Australian  
385 Research Council (grant number LP-0669240).

## REFERENCES

- Aasama K, Söber A, Rahi M. (2001)** Leaf anatomical characteristics associated with shoot hydraulic conductance, stomatal conductance and stomatal sensitivity to changes of leaf water status in temperate deciduous trees. *Australian Journal of Plant Physiology* **28**, 765-774.
- Anderson JE, Williams J, Kriedemann PE, Austin MP, Farquhar GD. 1996.** Correlations between carbon isotope discrimination and climate of native habitats for diverse eucalypt taxa growing in a common garden. *Australian Journal of Plant Physiology* **23**, 311-320.
- Assmann SM, Grantz DA. 1990.** Stomatal response to humidity in sugarcane and soybean: effect of vapour pressure difference on the kinetics of the blue light response. *Plant, Cell and Environment* **13**, 163-169.
- Barbour MM, Cernusak LA, Whitehead D, Griffin KL, Turnbull MH, Tissue DT, Farquhar GD. 2005.** Nocturnal stomatal conductance and implications for modelling delta  $\delta^{18}\text{O}$  of leaf-respired  $\text{CO}_2$  in temperate tree species. *Functional Plant Biology* **32**, 1107-1121.
- Barbour MM, Buckley TN. 2007.** The stomatal response to evaporative demand persists at night in *Ricinus communis* plants with high nocturnal conductance. *Plant, Cell and Environment* **30**, 711-721.
- Benyon RG. 1999.** Nighttime water use in an irrigated *Eucalyptus grandis* plantation. *Tree Physiology* **19**, 853-859.
- Brodribb TJ, Field TS, Jordan GS. 2007.** Leaf maximum photosynthetic rate and venation are linked by hydraulics. *Plant Physiology* **144**, 1890-1898.
- Brodribb TJ, McAdam S. A. M., Jordan GJ, Field TS. 2009.** Evolution of stomatal responsiveness to  $\text{CO}_2$  and optimisation of water-use efficiency among land plants. *New Phytologist*. **183**, 839-847.
- Bucci SJ, Goldstein G, Meinzer FC, Franco AC, Campanello P, Scholz FG. 2005.** Mechanisms contributing to seasonal homeostasis of minimum leaf water potential and predawn disequilibrium between soil and plant water potential in neotropical savanna trees. *Trees-Structure and Function* **19**, 296-304.
- Burghardt M, Riederer M. 2003.** Ecophysiological relevance of cuticular transpiration of deciduous and evergreen plants in relation to stomatal closure and leaf water potential. *Journal of Experimental Botany* **54**, 1941-1949.
- Caird MA, Richards JH, Donovan LA. 2007.** Nighttime stomatal conductance and transpiration in  $\text{C}_3$  and  $\text{C}_4$  plants. *Plant Physiology* **143**, 4-10.
- Cowan IR. 1977.** Stomatal behaviour and environment. *Advances in Botanical Research* **4**, 117-228.
- Daley MJ, Phillips NG. 2006.** Interspecific variation in nighttime transpiration and stomatal conductance in a mixed New England deciduous forest. *Tree Physiology* **26**, 411-419.
- Dawson TE, Pate JS. 1996.** Seasonal water uptake and movement in the root systems of Australian phreatophytic plants of dimorphic root morphology: A stable isotope investigation. *Oecologia* **107**, 13-20.
- Dawson TE, Burgess SSO, Tu KP, Oliveira RS, Santiago LS, Fisher JB, Simonin KA, Ambrose AR. 2007.** Nighttime transpiration in woody plants from contrasting ecosystems. *Tree Physiology* **27**, 561-575.
- Ehrler WL. 1971.** Periodic nocturnal stomatal opening of citrus in a steady environment. *Physiologia Plantarum* **25**, 488-&.

- Farquhar GD, Caemmerer SV, Berry JA.** 1980. A biochemical model of photosynthetic CO<sub>2</sub> assimilation in leaves of C<sub>3</sub> species. *Planta* **149**, 78-90.
- Farquhar GD, Schulze ED, Kupperts M.** 1980. Responses to humidity by stomata of *Nicotina glauca* L. and *Corylus avellana* L. are consistent with the optimization of carbon dioxide uptake with respect to water loss. *Australian Journal of Plant Physiology* **7**, 315-327.
- Field CB, Mooney HA.** 1986. The photosynthetic-nitrogen relationship in wild plants. In: Givnish TJ, ed. *On the economy of plant form and function*. Cambridge: Cambridge University Press, pp. 22-55.
- Franks PJ.** 2006. Higher rates of leaf gas exchange are associated with higher leaf hydrodynamic pressure gradients. *Plant Cell and Environment* **29**, 584-592.
- Franks PJ, Farquhar GD.** 1999. A relationship between humidity response, growth form and photosynthetic operating point in C<sub>3</sub> plants. *Plant, Cell and Environment* **22**, 1337-1349.
- Franks PJ, Farquhar GD.** 2007. The mechanical diversity of stomata and its significance in gas-exchange control. *Plant Physiology* **143**, 78-87.
- Franks PJ, Beerling DJ.** 2009. CO<sub>2</sub>-forced evolution of plant gas exchange capacity and water-use efficiency over the Phanerozoic. *Geobiology* **7**, 227-236.
- Franks PJ, Drake PL, Beerling DJ.** 2009. Plasticity in maximum stomatal conductance constrained by negative correlation between stomatal size and density: an analysis using *Eucalyptus globulus*. *Plant Cell and Environment* **32**, 1737-1748.
- Grantz DA, Zeiger E.** 1986. Stomatal responses to light and leaf-air water vapour pressure differences show similar kinetics in sugarcane and soybean. *Plant Physiology* **81**, 865-868.
- Groom PK, Froend RH, Mattiske EM.** 2001. Long-term changes in vigour and distribution of *Banksia* and *Melaleuca* overstorey species on the Swan Coastal Plain. *Journal of the Royal Society of Western Australia* **84**, 63-69.
- Groom PK.** 2002. Seedling water stress response of two sandplain *Banksia* species differing in ability to tolerate drought. *Journal of Mediterranean Ecology* **3**, 3-9.
- Groom PK.** 2004. Seedling growth and physiological response of two sandplain *Banksia* species differing in flood tolerance. *Journal of the Royal Society of Western Australia* **87**, 115-121.
- Harley PC, Thomas RB, Reynolds JF, Strain BR.** 1992. Modelling photosynthesis of cotton grown in elevated CO<sub>2</sub>. *Plant, Cell and Environment* **15**, 271-282.
- Hetherington AM, Woodward FI.** 2003. The role of stomata in sensing and driving environmental change. *Nature* **424**, 901-908.
- Hinckley TM, Duhme F, Hinckley AR, Richter H.** 1980. Water relations of drought-hardy shrubs: Osmotic potential and stomatal reactivity. *Plant Cell and Environment* **3**, 131-140.
- Jones HG.** 1992. *Plants and Microclimate*. Cambridge: Cambridge University Press.
- Körner C.** 1995. Leaf diffusive conductances in the major vegetation types of the globe. In: Schulz E-D, Caldwell MM, eds. *Ecophysiology of Photosynthesis*. Berlin: Springer-Verlag, 463-490.
- Lam A, Froend RH, Downes S, Loomes R.** 2004. Water availability and plant response: Identifying the water requirements of *Banksia* woodland on the Gngangara Groundwater Mound. A report to the Water Corporation of Western Australia.
- McDowell N, Pockman WT, Allen CD, Breshears DD, Cobb N, Kolb T, Plaut J, Sperry J, West A, Williams DG, Yezzer EA.** 2008. Mechanisms of plant survival and mortality during drought: why do some plants survive while others succumb to drought? *New Phytologist* **178**, 719-739.



- Meinzer FC.** 2003. Functional convergence in plant responses to the environment. *Oecologia* **134**, 1-11.
- Novick KA, Oren R, Stoy PC, Siqueira MBS, Katul GG.** 2009. Nocturnal evapotranspiration in eddy-covariance records from three co-located ecosystems in the Southeastern US: Implications for annual fluxes. *Agricultural and Forest Meteorology* **149**, 1491-1504.
- Pate JS, Jeschke WD, Aylward MJ.** 1995. Hydraulic Architecture and Xylem Structure of the Dimorphic Root Systems of South-West Australian Species of Proteaceae. *Journal of Experimental Botany* **46**, 907-915.
- Schulze ED, Kelliher FM, Körner C, Lloyd J, Leuning R.** 1994. Relationships among maximum stomatal conductance, ecosystem surface conductance, carbon assimilation rate, and plant nitrogen nutrition- A global ecology scaling exercise. *Annual Review of Ecology and Systematics* **25**, 629-660.
- Sharkey TD.** 1985. Photosynthesis in intact leaves of C<sub>3</sub> plants: physics, physiology and rate limitations. *The Botanical Review* **51**, 53-105.
- Snyder KA, Richards JH, Donovan LA.** 2003. Night-time conductance in C<sub>3</sub> and C<sub>4</sub> species: do plants lose water at night? *Journal of Experimental Botany* **54**, 861-865.
- Vico G, Manzoni S, Palmroth S, Katul G.** 2011. Effects of stomatal delays on the economics of leaf gas exchange under intermittent light regimes. *New Phytologist* **192**, 640-652.
- von Caemmerer S, Farquhar GD.** 1981. Some relationships between the biochemistry of photosynthesis and the gas exchange of leaves. *Planta* **153**, 376-387.
- Wong SC, Cowan IR, Farquhar GD.** 1979. Stomatal conductance correlates with photosynthetic capacity. *Nature* **282**, 424-426.
- Wullschleger SD.** 1993. Biochemical limitations to carbon assimilation in C<sub>3</sub> plants - a retrospective analysis of the A/c<sub>i</sub> curves from 109 Species. *Journal of Experimental Botany* **44**, 907-920.
- Zencich SJ, Froend RH, Turner JV, Gailitis V.** 2002. Influence of groundwater depth on the seasonal water sources of water accessed by *Banksia* tree species on a shallow, sandy coastal aquifer. *Oecologia* **131**, 8-19.

**Table 1.** Approximate range in groundwater depth of the study species

Species	Approximate range of groundwater depth (m)	Source
<i>Banksia attenuata</i>	3 to > 30	Zencich <i>et al.</i> , 2002; Lam <i>et al.</i> , 2004
<i>Banksia menziesii</i>	3 to > 30	Lam <i>et al.</i> , 2004)
<i>Banksia prionotes</i>	1.5 to 10	Dawson and Pate, 1996; Pate <i>et al.</i> , 1995
<i>Banksia ilicifolia</i>	< 10	Groom <i>et al.</i> , 2001; Zencich <i>et al.</i> , 2002
<i>Banksia littoralis</i>	< 5	Groom <i>et al.</i> , 2001

**Table 2.** Comparison of stomatal conductances to water vapour ( $\text{mmol m}^{-2} \text{s}^{-1}$ ) in the five *Banksia* species studied:  $g_{\text{min(dawn)}}$ , prior to morning light exposure;  $g_{\text{op}}$ , at full stomatal opening under ideal conditions;  $g_{\text{min(day)}}$ , following closure in response to leaf darkening at midday;  $g_{\text{min(abs)}}$ , after leaf excision. Numbers are means with standard error in brackets.

Species	$g_{\text{min(dawn)}}$	$g_{\text{op}}$	$g_{\text{min(day)}}$	$g_{\text{min(abs)}}$
<i>B. attenuata</i>	9.42 (1.9)	345 (20)	120 (19)	5.7 (0.8)
<i>B. menziesii</i>	6.03 (0.7)	356 (34)	135 (25)	9.5 (0.8)
<i>B. illicifolia</i>	12.4 (1.8)	421 (32)	143 (23)	8.5 (2.7)
<i>B. prionotes</i>	12.9 (1.1)	469 (4)	171 (20)	8.8 (0.7)
<i>B. littoralis</i>	44.0 (2.9)	761 (19)	95 (4)	20 (0.7)

## FIGURE LEGENDS

**Figure 1.** The different phases of stomatal conductance examined in this study:  $g_{\min}$ , steady state stomatal conductance in darkness, either at dawn ( $g_{\min(\text{dawn})}$ ) or after suddenly induced darkness ( $g_{\min(\text{day})}$ );  $(dg/dt)_{\max}$ , the maximum rate of change of  $g$  during light-induced stomatal opening;  $g_{\text{op}}$ , steady state operating stomatal conductance under standardised ideal conditions (see Methods);  $t_{50}$ , time taken to reach 50% of the range between  $g_{\min}$  and  $g_{\text{op}}$ ;  $g_{\min(\text{abs})}$ ; the absolute minimum steady-state stomatal conductance after leaf excision, assumed to result from zero turgor in stomatal guard cells.

**Figure 2.** Idealized distribution of *Banksia* species on the Gngangara Groundwater Mound with respect to depth to groundwater (see Table 1) and unsaturated soil volume. *Banksia littoralis* only occurs in association with watercourses and wetland habitats and are excluded from dune crests occupied by *Banksia attenuata* and *Banksia menzeisii*. Accordingly, *B. littoralis* has a highly restricted geographical distribution, while *B. attenuata* and *B. menzeisii* have a more extensive geographical distribution encompassing several hydrological habitats. Adapted from Lam *et al.*, 2004. Inset: Illustrating the range of leaf size and shape across the study species.

**Figure 3.** Relationship between  $g_{\text{op}}$ ,  $g_{\min(\text{dawn})}$  and  $(dg/dt)_{\max}$ . (A) Across individuals,  $g_{\text{op}}$  was positively correlated with  $g_{\min(\text{dawn})}$ . Each point represents the mean  $\pm$  S.E. of  $n = 6$  consecutive steady-state records for an individual plant. The maximum rate of stomatal opening  $(dg/dt)_{\max}$  was positively correlated with maximum steady-state stomatal conductance,  $g_{\text{op}}$  (B) and minimum stomatal conductance induced by darkness,  $g_{\min(\text{day})}$  (C).

**Figure 4.** Smaller, faster stomata. The maximum rate of stomatal opening  $(dg/dt)_{\max}$  was negatively correlated with maximum stomatal size,  $S$  (panel A) and positively correlated with stomatal density  $D$ , (panel B). The time to reach 50% of the range between  $g_{\min(\text{dawn})}$  and  $g_{\text{op}}$  ( $t_{50}$ ) was positively correlated with stomatal size (panel C).

**Figure 5.** Time-series of stomatal opening and CO<sub>2</sub> assimilation rate in response to light. Each point is the mean  $\pm$  S.E. stomatal conductance ( $g$ , panels A-E) and assimilation rate ( $A$ , panels F-J) measured at discrete time intervals ( $n = 4$  plants per species). The letter “I” in each graph indicates the start of the illumination phase, when leaves were exposed to a PAR of 1500  $\mu\text{mol m}^{-2} \text{s}^{-1}$ . Prior to this point leaves were darkened (PAR = 0  $\mu\text{mol m}^{-2} \text{s}^{-1}$ ).

**Figure 6.** Relationship between CO<sub>2</sub> assimilation rate, stomatal conductance and instantaneous water use efficiency. Panel (A), instantaneous CO<sub>2</sub> assimilation rate  $A$  versus instantaneous stomatal conductance  $g$ ; panel (B), instantaneous water-use efficiency  $\text{WUE}_i$  versus  $g$ . Note the peak in  $\text{WUE}_i$  at around the same  $A$  for all species (approximately 5  $\mu\text{mol m}^{-2} \text{s}^{-1}$ ); panel (C), negative correlation between  $\text{WUE}_i$  and steady state operating stomatal conductance,  $g_{\text{op}}$ .

**Figure 7.** The maximum (operating) photosynthetic rate  $A_{op}$  was positively correlated with the maximum rate of carboxylation,  $V_{c_{max}}$  (panel A) and the light saturated rate of electron transport,  $J_{max}$  (panel B).

**Figure 8.** Incomplete stomatal closure in the dark. Following a sudden transition from 1500 to 0 PAR (indicated by the arrow labelled “dark”), stomatal conductance ( $g$ ) declined to a steady state minimum ( $g_{min(day)}$ , see Fig. 1). Further reduction in  $g$  occurred after leaf excision (indicated by the arrow), reaching the absolute minimum conductance ( $g_{min(abs)}$ ) after desiccation induced the complete loss of guard cell turgor. Panels A-E show the time series of  $g$  for each species (mean  $\pm$  S.E.,  $n = 4$  plants per species).

**Figure 9.** Simulations based on the data and model in (Franks PJ, 2006) show that following an increase in evaporative demand (leaf-to-air vapour pressure difference, VPD), plants that operate with higher stomatal conductance  $g_{op}$  are exposed to larger water potential gradients (shown here for leaves,  $\Delta\Psi_{leaf}$ ; A), even though they have inherently larger maximum leaf hydraulic conductance  $k_{leaf(max)}$  (B). For illustrative purposes two operating stomatal conductances are contrasted with one another (0.10 and 0.20 mol m<sup>-2</sup> s<sup>-1</sup> at 1 kPa VPD), with their initial and final values indicated by the start and end point (respectively) of the arrows. Faster response time reduces the duration of exposure to excessive water potential gradients.

Figure 1

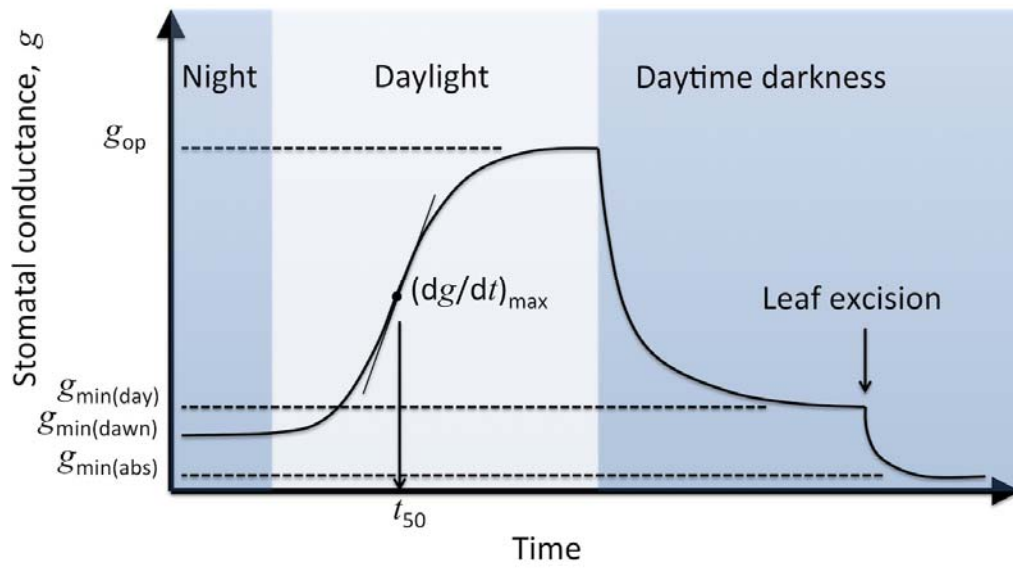


Figure 2

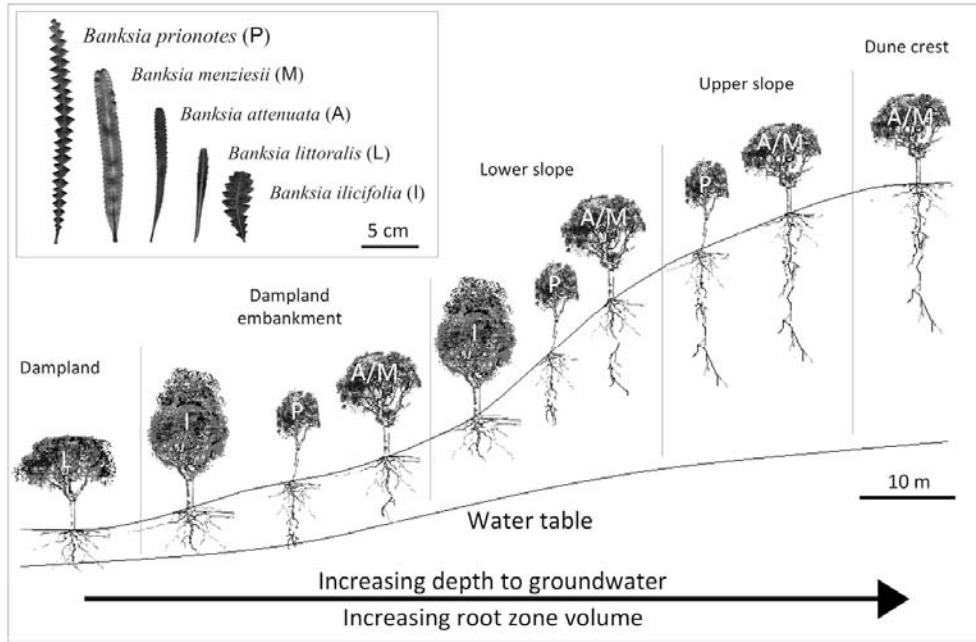


Figure 3

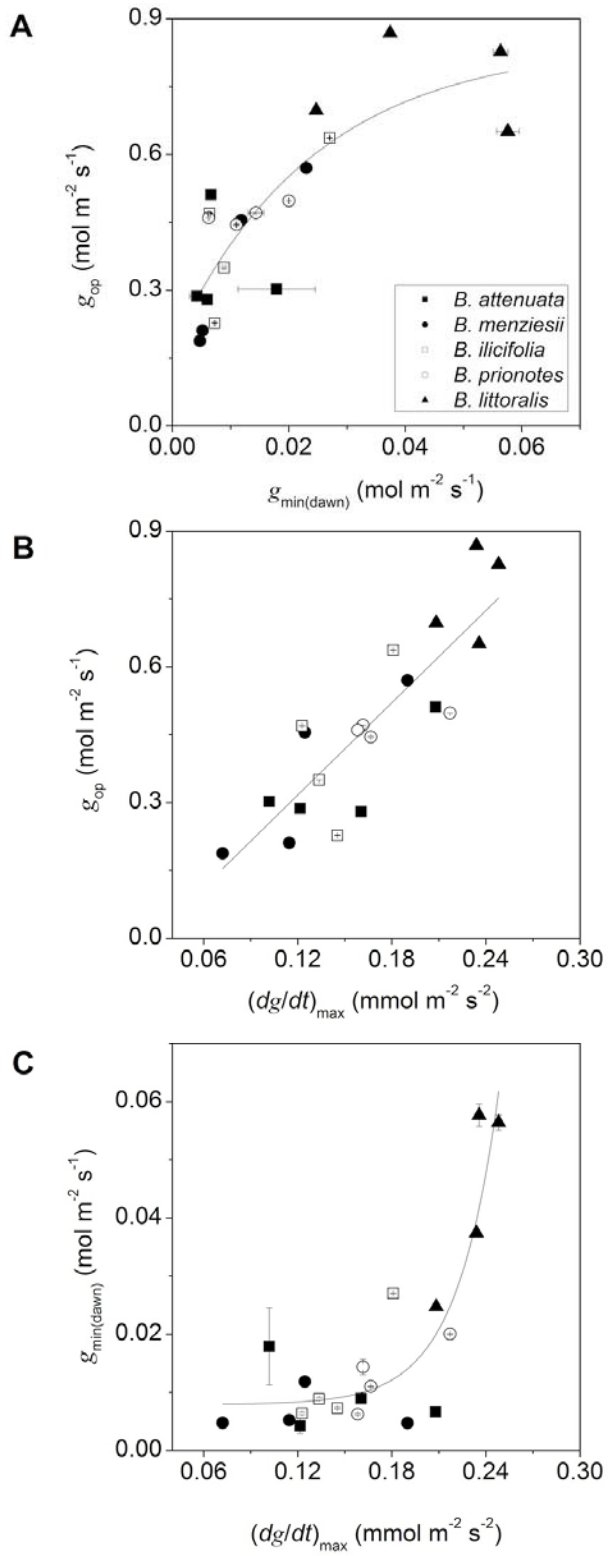




Figure 4

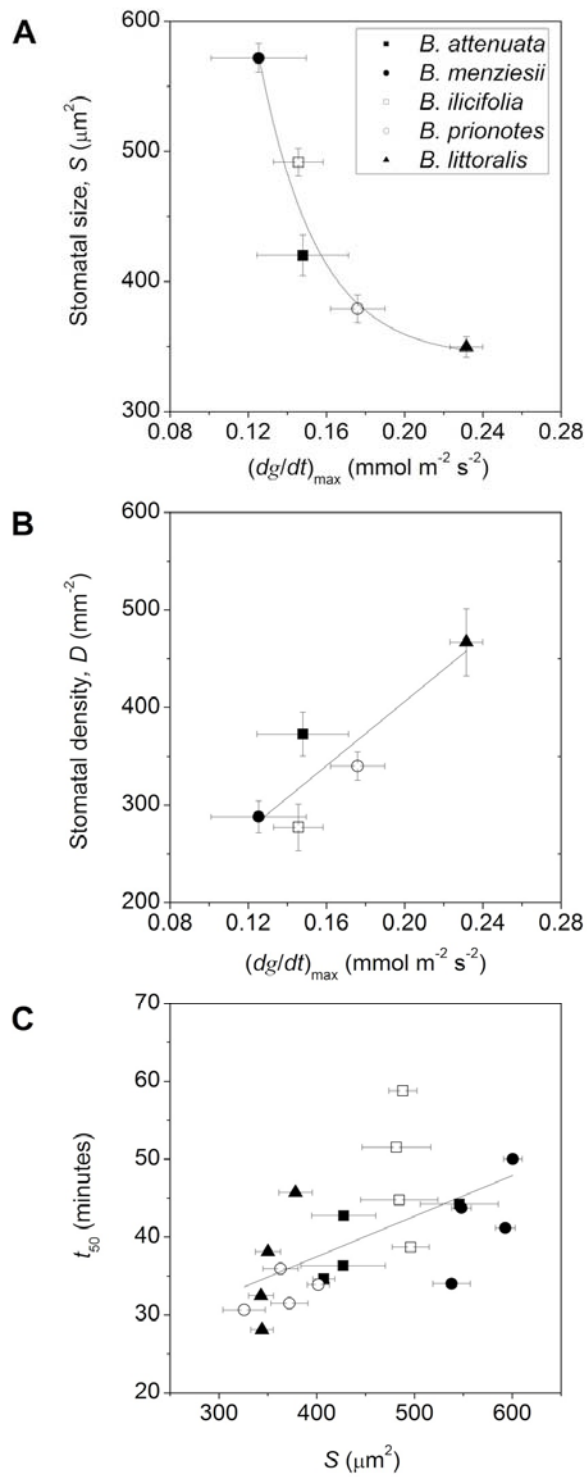


Figure 5

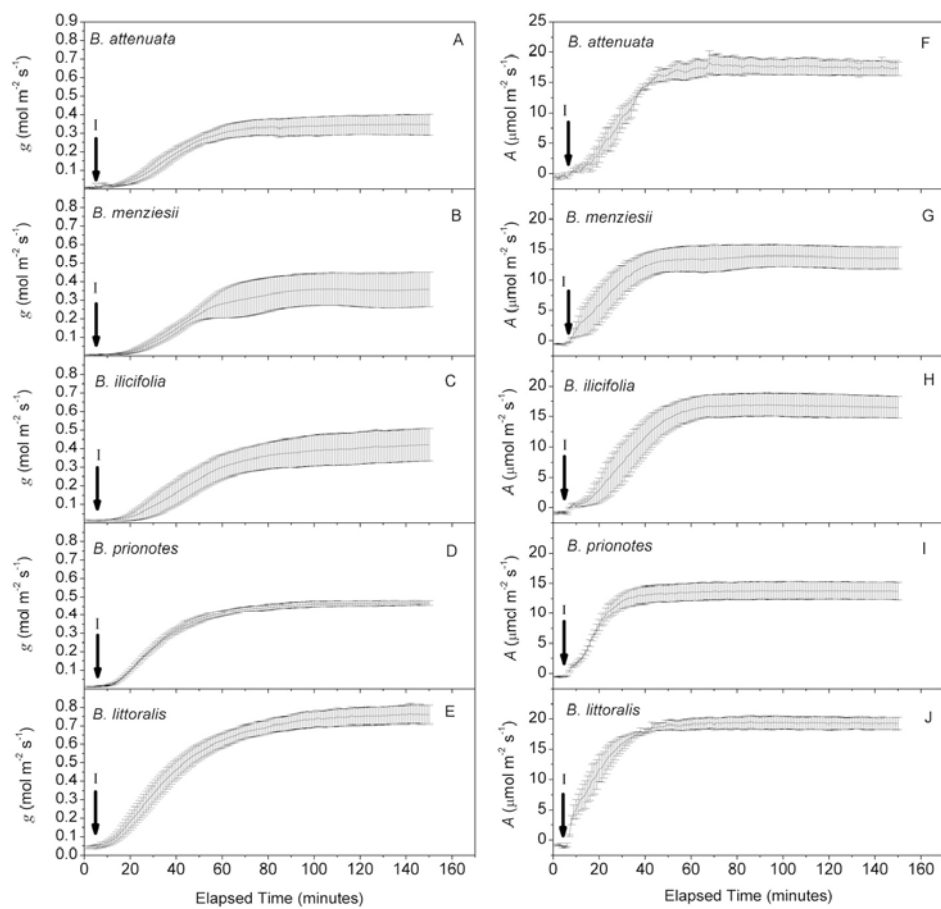


Figure 6

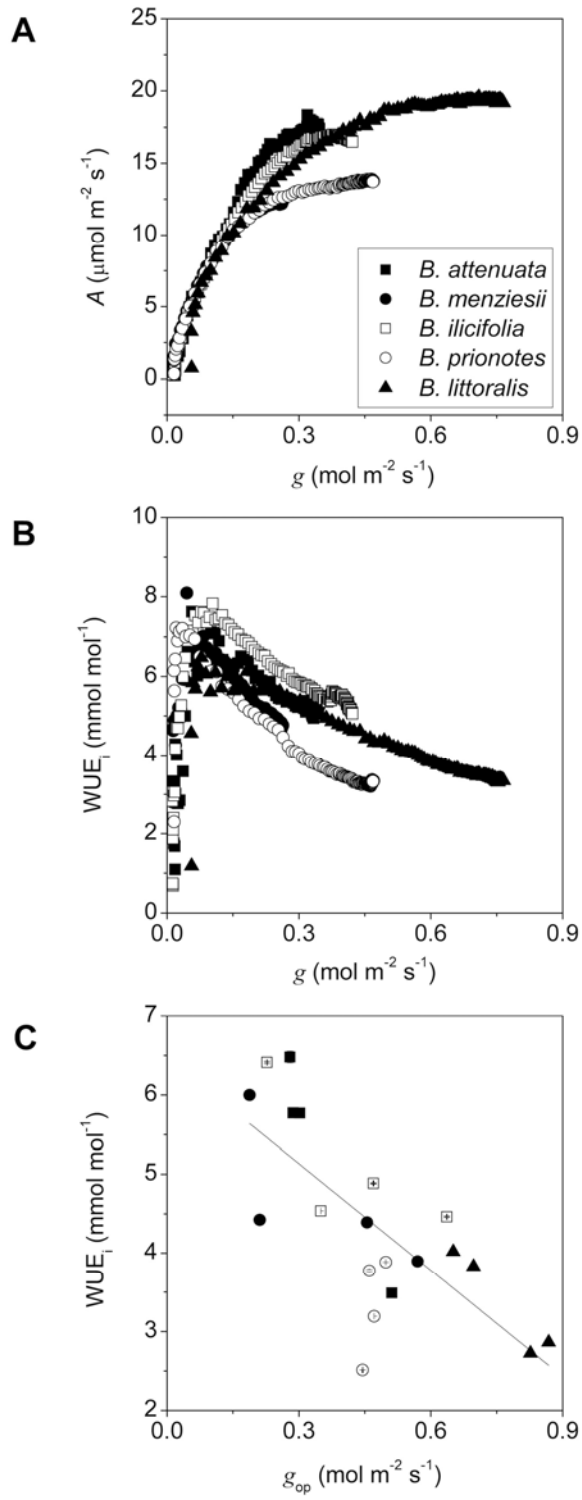


Figure 7

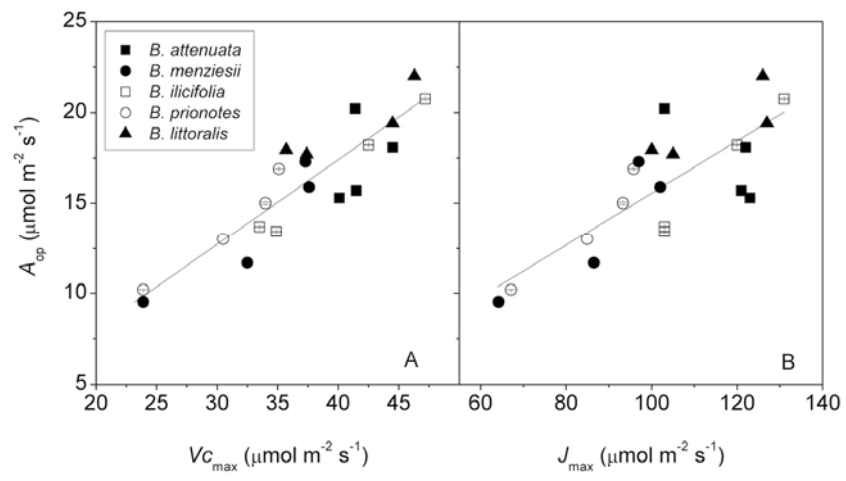


Figure 8

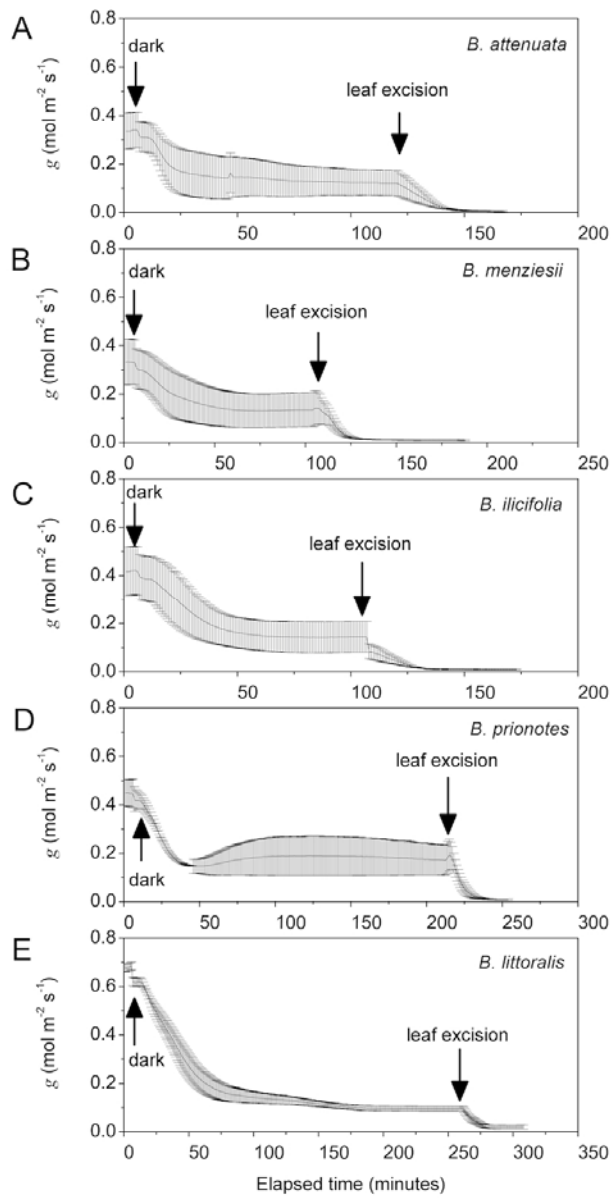


Figure 9

